Cooper, A.K., O'Brien, P.E., and Richter, C. (Eds.)
Proceedings of the Ocean Drilling Program, Scientific Results Volume 188

6. Data Report: Quaternary–Pliocene Diatom Biostratigraphy of ODP Sites 1165 and 1166, Cooperation Sea and Prydz Bay[1]

Jason M. Whitehead[2] and Steven M. Bohaty[3]

ABSTRACT

The biostratigraphic distribution and qualitative relative abundance of Quaternary–Pliocene diatoms from Ocean Drilling Program Leg 188, Sites 1165 (64.380°S, 67.219°E) and 1166 (67.696°S, 74.787°E) offshore from East Antarctica, are documented in this report. The upper ~50 meters below seafloor (mbsf) of Hole 1165B consists of brown diatom-bearing silty clay spanning the upper Pleistocene to lower Pliocene. The diatom stratigraphy indicates a disconformity at ~17.1 mbsf of 0.5- to 0.6-m.y. duration. The integration of biostratigraphic and magneto-stratigraphic data identified other disconformities at ~6.0, 14.4, 15.6, and 16.0 mbsf, but the duration of these hiatuses cannot be resolved through diatom biostratigraphy. In Hole 1166A, a narrow interval of diatomaceous Quaternary sediment is identified in the upper 2.92 mbsf and dated biostratigraphically at <0.38 Ma. The remaining Quaternary–Pliocene section is dominated by diamicton, except at ~114 mbsf, where two thin diatomaceous beds are present. The lower bed is ~65 cm thick, 2.5–2.7 to 2.7–3.2 Ma in age, and possibly disconformably overlain by the upper bed, which is ~15 cm thick and 1.8–2.0 to 2.1–2.5 Ma in age. The Pliocene assemblages in Hole 1166A contain components of both Southern Ocean and Antarctic continental shelf (Ross Sea) diatom floras.

[1]Whitehead, J.M., and Bohaty, S.M., 2003. Data report: Quaternary–Pliocene diatom biostratigraphy of ODP Sites 1165 and 1166, Cooperation Sea and Prydz Bay. *In* Cooper, A.K., O'Brien, P.E., and Richter, C. (Eds.), *Proc. ODP, Sci. Results,* 188, 1–25 [Online]. Available from World Wide Web: <http://www-odp.tamu.edu/publications/188_SR/VOLUME/CHAPTERS/008.PDF>. [Cited YYYY-MM-DD]
[2]Department of Geology, 214 Bessey Hall, University of Nebraska, Lincoln NE 68588-0340, USA.
jm_whitehead@hotmail.com
[3]Earth Sciences Department, University of California, Santa Cruz, Santa Cruz CA 95064, USA.

Initial receipt: 18 July 2002
Acceptance: 16 December 2002
Web publication: 12 March 2003
Ms 188SR-008

INTRODUCTION

Ocean Drilling Program (ODP) Site 1165 (64.380°S, 67.219°E) (Fig. F1) is located in the Cooperation Sea region of the Southern Ocean, on the Antarctic continental rise, offshore from Prydz Bay and centered over the Wild Drift (Shipboard Scientific Party, 2001). The Wild Drift is an elongate sediment body formed by the interaction of terrigenous sediment from the Antarctic continental shelf, ocean currents, and pelagic siliceous ooze (notably diatoms and silicoflagellates) "raining out" from the overlying water column.

Farther landward, ODP Site 1166 (67.696°S, 74.787°E) (Fig. F1) is located on the continental shelf in Prydz Bay. The bay is at the seaward edge of the Lambert Graben, which may have first formed in the Permian but is now largely occupied by the Amery Ice Shelf (Stagg, 1985). The graben is a conduit for ice draining from the largest catchment area in East Antarctica (Hambrey et al., 1991). Seismic data from the Prydz Bay continental shelf and ODP Leg 119 drilling results indicate here there is a seaward prograding sequence of Paleogene glaciomarine sediments overlain by Neogene glacial sediments up to 300 m in thickness (Hambrey et al., 1991).

In situ Pliocene diatom-bearing marine strata are uncommon in the Prydz Bay–Lambert Graben region. A Pliocene diatomite bed (~60 cm thick) is present within diamicts at ODP Site 742 (Fig. F1) (Mahood and Barron, 1996). Diatomaceous Pliocene strata are exposed in the Vestfold Hills (Sørsdal Formation) (Harwood et al., 2000) and Larsemann Hills (McMinn and Harwood, 1995), and Pliocene–Pleistocene strata outcrop 250 km inland of the current Amery Ice Shelf edge in the Amery Oasis (Bardin Bluffs Formation) (Whitehead and McKelvey, 2001) (Fig. F1). Reworked Pliocene and Pleistocene diatoms have also been recovered from Quaternary sediments in Prydz Bay (Domack et al., 1998). In situ Quaternary diatomaceous marine strata in Prydz Bay are generally present as a thin veneer, a few meters thick, on the seafloor or as thin beds within glacial sediments and have been dated primarily using radiocarbon techniques (Domack et al., 1991, 1998; Taylor and McMinn, 2002). Detailed sediment and diatom studies have not been undertaken on the Wild Drift site prior to Leg 188.

Previous Deep Sea Drilling Project and ODP legs have sequentially improved the diatom biostratigraphic framework of the Southern Ocean (e.g., Abbott, 1974; McCollum, 1975; Schrader, 1976; Ciesielski, 1983; Gersonde and Burckle, 1990; Baldauf and Barron 1991; Harwood and Maruyama, 1992; Gersonde and Bárcena, 1998; Zielinski and Gersonde, 2002). The Quaternary–Pliocene diatom biostratigraphy of the Antarctic continental shelf has been largely developed in the Ross Sea and closely corresponds to the Southern Ocean biostratigraphic framework, allowing for direct comparisons with a few regional differences (Winter and Harwood, 1997). Both Southern Ocean and Antarctic Shelf diatom zonations have been applied to the sediments from Sites 1165 and 1166.

METHODS

Ship- and shore-based biostratigraphic analyses were performed on smear slides mounted with Norland optical adhesive #61 (refractive index = 1.56) from Hole 1165B (0.00–54.39 meters below seafloor [mbsf]) and Hole 1166A (0.00–1164 mbsf). Diatom identification was carried

F1. Locations referred to in this report, p. 18.

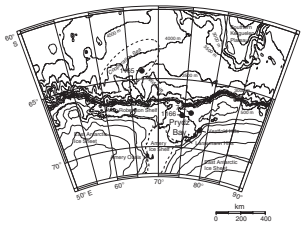

out using an Olympus BH-2 light microscope at 1000× magnification (oil-immersion objective). Preliminary biostratigraphic analyses were undertaken on core catcher samples to identify the important diatom datums. Diatom datums and zonal boundaries were then constrained using detailed sample intervals at ~10-cm increments, where possible. The calibrated ages for the marker species datums have been recalculated to the timescale of Berggren et al. (1995) (Table T1). Magnetostratigraphic analysis of the cores is reported by Florindo et al. (in press), and the polarity reversals are tied to the geomagnetic timescale using radiolarian and diatom datums.

T1. Primary diatom datums, Holes 1165B and 1166A, p. 19.

The slides were systematically scanned, and qualitative diatom occurrence data collected (Tables T2, T3). The abundance of individual diatom taxa was based on the number of specimens observed per field of view at 1000× and recorded as follows:

T2. Diatom occurrence, Hole 1165B, p. 20.

T3. Diatom occurrence, Hole 1166A, p. 21.

A = abundant (>10 valves per field of view).
C = common (1–10 valves per field of view).
F = few (≤1 valve per 10 fields of view and <1 valve per field of view).
R = rare (3 valves per traverse of coverslip and <1 valve per 10 fields of view).

Those taxa whose abundance has been recorded in italics and accompanied by an "r" (e.g., *Xr*) are out of their known biostratigraphic ranges and have been interpreted as reworked.

Similar categories (i.e., A, C, F, and R) were used to assess the "overall abundance" of diatoms in each sample, with the addition of an extra category:

Tr = trace (at least 1 valve per slide).

Preservation was qualitatively assessed from the degree of mechanical breakage and apparent where

G = good (slight to no fragmentation and/or dissolution).
M = moderate (moderate fragmentation and/or dissolution).
P = poor (severe effects of fragmentation and/or dissolution).

RESULTS

The Hole 1165B diatom assemblages are poorly preserved above ~17.0 mbsf. Diatom preservation and abundance is moderate between 17.0 and 35.0 mbsf and optimal between ~30.0 and 50.0 mbsf. The stratigraphic position of the primary diatom datum events and occurrence data for Holes 1165B and 1166A are tabulated in Tables T1, T2, and T3. The biostratigraphic ages have been revised to the Berggren et al. (1995) timescale, and supporting references are cited. Many sample intervals in Hole 1165B contain notable trace occurrences of reworked diatom species, which include numerous Pliocene, Miocene, and Oligocene taxa (Table T4).

T4. Reworked diatoms, Hole 1165B, p. 23.

INTERPRETATION

Hole 1165B

The Southern Ocean zonal scheme of Harwood and Maruyama (1992) applies directly to the Quaternary and Pliocene section in Hole 1165B. The last occurrence (LO) of *Actinocyclus ingens* Rattray occurs between Samples 188-1165B-1H-2, 20–21 cm (1.70 mbsf), and 1H-4, 20–21 cm (4.70 mbsf), placing the base of the *Thalassiosira lentiginosa* Zone at 4.70 mbsf. A poorly preserved interval between 1.70 and 4.70 mbsf prevents the zonal boundary from being constrained to a narrow stratigraphic interval. An age of <0.38 Ma (Zielinski and Gersonde, 2002) is therefore interpreted above 1.70 mbsf based on the absence of *A. ingens*.

The interval between 4.70 and 8.50 mbsf is assigned to the *A. ingens* Zone based on the presence of *A. ingens* and absence of *Fragilariopsis barronii* (Gersonde) Gersonde and Bárcena. The base of the *A. ingens* Zone is marked by the LO of *F. barronii* between Samples 188-1165B-2H-2, 20–21 cm (6.81 mbsf), and 2H-2, 95–96 cm (8.50 mbsf). The identification of the LO of *F. barronii* is difficult because of taxonomic difficulties in identifying this taxon (also noted by Gersonde and Bárcena, 1998). *F. barronii* sensu stricto contains considerable phenotypic variation, as illustrated in Gersonde, 1991. Harwood and Maruyama (1992) illustrate two forms of *F. barronii,* which may encompass the end-members of the transitional *F.* sp. cf. *barronii* also observed in Hole 1165B.

The interval between 9.25 and 17.25 mbsf is characterized by poor diatom preservation and low abundance and has been left unzoned. The LO of *Thalassiosira kolbei* (Jousé) Gersonde is noted between Samples 188-1165B-3H-1, 77–80 cm (17.07 mbsf), and 3H-1, 95–96 cm (17.25 mbsf). However, because of the poor preservation of the samples between 9.25 and 17.25 mbsf the stratigraphic position of this datum may be compromised by preservational factors. This LO datum of *T. kolbei* consistently occurs within Subchron C2n (Baldauf and Barron, 1991; Harwood and Maruyama, 1992) (Table **T2**).

The LO of *Thalassiosira vulnifica* (Gombos) Fenner also occurs between Samples 188-1165B-3H-1, 77–80 cm (17.07 mbsf), and 3H-1, 95–96 cm (17.25 mbsf). The co-occurrence of *Fragilariopsis weaveri* (Ciesielski) Gersonde and Bárcena in Sample 188-1165B-3H-1, 95–96 cm (17.25 mbsf), suggests there is a disconformity of 0.5- to 0.6-m.y duration at this level, based on the absence of the *T. vulnifica* Zone and *Thalassiosira insigna–T. vulnifica* Subzone "b." Samples 188-1165B-3H-1, 117–120 cm (17.25 mbsf), through 3H-CC, 0–5 cm (25.01 mbsf), are assigned to the *T. insigna–T. vulnifica* Subzone "a" (2.5–2.7 to 3.2 Ma). This zone is constrained by the presence of *T. vulnifica, F. weaveri,* and *T. insigna* (Jousé) Harwood and Maruyama in this interval. The first occurrence (FO) of *T. vulnifica* is identified between Samples 188-1165B-3H-CC (25.01 mbsf) and 4H-1, 6.0–8.5 cm (25.86 mbsf).

The FO of *Fragilariopsis interfrigidaria* (McCollum) Gersonde and Bárcena is identified between Samples 188-1165B-5H-2, 127–129.5 cm (38.07 mbsf), and 5H-3, 95–96 cm (39.25 mbsf). The *F. interfrigidaria* Zone (2.7–3.2 to 3.7–3.8 Ma) is placed between Samples 188-1165B-3H-CC, 0–5 cm (25.01 mbsf), and 5H-2, 127–129.5 cm (38.07 mbsf), based on the presence of *F. interfrigidaria* and the absence of *T. vulnifica*. The boundary between the upper and lower Pliocene lies within the *F. interfrigidaria* Zone and is placed at 36.46 mbsf (at the base of the Subchron C2An.3n) (Florindo et al., in press). The FO of *F. barronii* is noted between Samples 188-1165B-5H-5, 47–50 cm (41.77 mbsf), and 5H-5, 60–

61 cm (41.90 mbsf). Therefore, the interval between 38.07 and 41.77 mbsf is placed within the *F. barronii* Zone, which is constrained by the presence of *F. barronii* and the absence of *F. interfrigidaria*. Intermittent occurrence of the *F. barronii* subzonal marker species *Rhizosolenia costata* Gersonde at Site 1165 prevents subdivision of the *F. barronii* Zone into Subzones "a" and "b."

The FO of *Thalassiosira inura* Gersonde occurs between Samples 188-1165B-6H-4, 95–96 cm (50.25 mbsf), and 6H-5, 59–60 cm (51.39 mbsf). The interval 41.77–50.35 mbsf is placed within the *T. inura* Zone (4.2–4.3 to 4.8–5.0 Ma) as indicated by the presence of *T. inura* and the absence of *F. barronii*. The interval below the FO of *T. inura* has been assigned to the *Thalassiosira oestrupii* Zone, based on the presence of *T. oestrupii* (Ostenfeld) Hasle and the absence of *T. inura*.

Hole 1166A

In Hole 1166A a narrow interval of diatomaceous Quaternary sediment was identified in the upper 3.02 m, biostratigraphically dated as <0.38 Ma from the absence of *A. ingens,* and assigned to the *T. lentiginosa* Zone. The underlying Quaternary–Pliocene section is dominated by diamicton, with the exception of two silty horizons at ~114 mbsf.

At ~114 mbsf, well-preserved and abundant upper Pliocene diatoms occur in two silt beds. In the upper silt bed (~113.95–114.10 mbsf), the presence of *T. kolbei* (Jousé) Gersonde (LO = 1.8–2.0 Ma) and the absence of *T. vulnifica* (Gombos) Fenner (LO = 2.1–2.5 Ma) indicates an age of 1.8–2.0 to 2.1–2.5 Ma. In the lower silt bed (~114.50–115.15 mbsf), the co-occurrence of *T. vulnifica* (FO = 2.7–3.2 Ma) and *T. insigna* (Jousé) Harwood and Maruyama (LO = 2.5–2.6 Ma) indicates an age of 2.5–2.7 to 2.7–3.2 Ma (Tables **T1, T3**).

The upper silt bed is assigned to the *T. kolbei* Zone using the Southern Ocean zonal scheme of Harwood and Maruyama (1992). This correlates to a similar Pliocene section recovered in Prydz Bay at Site 742 (Mahood and Barron, 1996). The lower silt bed in Hole 1166A has presently been left unzoned, however, because of inconsistencies between the application of the Southern Ocean zonal scheme (Harwood and Maruyama, 1992) and the Antarctic shelf zonal scheme (Winter and Harwood, 1997).

Application of the Southern Ocean zonal scheme of Harwood and Maruyama (1992) indicates a disconformity occurs between the two silt beds, but the application of the Antarctic Shelf zonal scheme of Winter and Harwood (1997) indicates the beds are conformable. The conflict between zonal schemes arises from the biostratigraphic application of the LO of *T. insigna*. The range of this species does not overlap with *T. vulnifica* in the Ross Sea but does so in the Southern Ocean (Winter and Harwood, 1997) and in Hole 1166A. *Thalassiosira elliptipora* (Donahue) Fenner also has a different range in the Ross Sea from that recorded from the Southern Ocean. In the Southern Ocean the FO of *T. elliptipora* occurs near the LO of *T. vulnifica,* but in the Ross Sea and at Prydz Bay Hole 1166A the biostratigraphic ranges of these species overlap.

DISCUSSION

Integration of diatom biostratigraphy with palaeomagnetic data (Florindo et al., in press) provides excellent age control through the Pliocene intervals of Holes 1165B and 1166A. The age of some datums

were recalculated from their stratigraphic position in Hole 1165B and a linear extrapolation of the ages between paleomagnetic reversals (Table T5). These age calibrations are in general agreement with previously published ages (e.g., Zielinski and Gersonde, 2002).

T5. Diatom datums, Hole 1165B, p. 25.

Hole 1165B

The close association between the sequence of biostratigraphic events at Site 1165 to the Southern Ocean diatom zonation of Harwood and Maruyama (1992) reflects the oceanic setting at this site. Pervasive reworking of diatoms is also evident through much of the Quaternary–Pliocene interval at Site 1165 (Table T4). This reworking may have occurred during enhanced water current flow and/or during glacial erosion of Neogene and Paleocene diatom-bearing marine sediments that are present inland, as inferred from remnants preserved in Prydz Bay, Mac.Robertson Shelf, Larsemann Hills, Vestfold Hills, and the Prince Charles Mountains (Baldauf and Barron, 1991; Barron and Mahood, 1993; McMinn and Harwood, 1995; Mahood and Barron, 1996; Quilty et al., 1999; Harwood et al., 2000; Whitehead, 2000; McKelvey et al., 2001; Whitehead and McKelvey, 2001). A continental shelf origin for some of this reworked material is indicated by the trace presence of benthic diatoms and siliceous sponge spicules (Table T4), which are abundant in shallow-water environments (Dunbar et al., 1989; Whitehead and McMinn, 1997).

Hole 1166A

At Site 1166, the Pliocene diatom assemblages contain continental shelf and open-ocean components and may reflect oceanic influences within the continental shelf setting of Prydz Bay. This is also evident amongst the modern surficial diatom assemblages in Prydz Bay, which contain an oceanic element that has entered the continental shelf via water pushed landward by the Prydz Bay gyre (Taylor et al., 1997). The differences between shelf and oceanic diatom zonations do not impact the age assignment of the upper bed of Pliocene strata at Site 1165. However, uncertainty about the presence of a disconformity between the beds prevented a concise palaeomagnetic age interpretation of the polarity reversed lower bed (Subchron C2r.1r or C2r.2r) (O'Brien, Cooper, Richter, et al., 2001). The upper Pliocene silt bed, assigned to the *T. kolbei* Zone, correlates to an upper Pliocene bed (~60 cm in thickness) identified ~100 km away within Hole 742A, at ~128 mbsf (Mahood and Barron, 1996). The narrow thickness (~15 cm) and depth (~114 mbsf) of this bed are similar to that at Site 742. Older Pliocene strata appear to be disconformably absent from Site 742, which further supports the presence of a disconformity between the Pliocene beds in Hole 1166A.

CONCLUSION

In summary, the Southern Ocean zonal scheme of Harwood and Maruyama (1992) applies directly to the Quaternary and Pliocene section in Hole 1165B. The upper ~50 mbsf of Hole 1165B consists of brown diatom-bearing silty clay (O'Brien, Cooper, Richter, et al., 2001) spanning the upper Pleistocene to lower Pliocene. The base of Subchron C1n is present at 5.37 mbsf, which suggests that there is at least one disconformity above this depth (O'Brien, Cooper, Richter, et al., 2001). A

disconformity (of ~1 m.y. duration) between upper Pleistocene and lower Pleistocene sediments was identified at ~6.0 mbsf, based on magnetostratigraphic data. The palaeomagnetic record also indicates that a series of closely spaced disconformities occur at 14.4, 15.6, and ~16.0 mbsf (O'Brien, Cooper, Richter, et al., 2001; Florindo et al., in press); however, the amount of missing time represented cannot be resolved with diatom biostratigraphy. The absence of the *T. vulnifica* Zone and *T. insigna–T. vulnifica* Subzone "b" suggests that there is a disconformity at ~17.1 mbsf of 0.5- to 0.6-m.y duration. In Hole 1166A, a narrow interval of diatomaceous Quaternary sediment was identified in the upper 2.92 mbsf and biostratigraphically dated at <0.38 Ma. The remaining Quaternary–Pliocene section is dominated by diamicton; however, at ~114 mbsf two diatomaceous Pliocene beds were identified. The lower bed is ~65 cm thick, 2.5–2.7 to 2.7–3.2 Ma in age, and possibly disconformably overlain by the upper bed. The upper bed is ~15 cm thick and 1.8–2.0 to 2.1–2.5 Ma in age.

ACKNOWLEDGMENTS

This research used samples and data provided by the Ocean Drilling Program (ODP). ODP is sponsored by the U.S. National Science Foundation (NSF) and participating countries under management of Joint Oceanographic Institutions (JOI) Inc. Funding for this research was provided by JOI/USSAC grant F001167/188F001233. We thank David Harwood (University of Nebraska-Lincoln), Frank Rack (Ocean Drilling Program), Alan Cooper (Stanford), Phillip O'Brien (Australian Geological Survey Organization), and Sarah Steele (Hamilton College) for enabling participation on Leg 188. We also thank our fellow cruise participants for their contributions. We thank the editor and reviewer for useful and thorough suggestions.

REFERENCES

Abbott, W.H., 1974. Temporal and spatial distribution of Pleistocene diatoms from the southeast Indian Ocean. *Nova Hedwigia Beih.,* 25:291–346.

Akiba, F., 1982. Late Quaternary diatom biostratigraphy of the Bellingshausen Sea, Antarctic Ocean. *Rep. Tech. Res., Cen. Jpn. Nat. Oil Corp.,* 16:31–74.

Baldauf, J.G., and Barron, J.A., 1991. Diatom biostratigraphy: Kerguelen Plateau and Prydz Bay regions of the Southern Ocean. *In* Barron, J., Larsen, B., et al., *Proc. ODP, Sci. Results,* 119: College Station, TX (Ocean Drilling Program), 547–598.

Barron, J.A., 1981. Marine diatom biostratigraphy of the Montesano Formation near Aberdeen, Washington. *Spec. Rep.—Geol. Soc. Am.,* 184:113–126.

————, 1985. Miocene to Holocene planktic diatoms. *In* Bolli, H.M., Saunders, J.B., and Perch-Nielsen, K. (Eds.), *Plankton Stratigraphy:* Cambridge (Cambridge Univ. Press), 763–809.

Barron, J.A., and Mahood, A.D., 1993. Exceptionally well-preserved early Oligocene diatoms from glacial sediments of Prydz Bay, East Antarctica. *Micropaleontology,* 39:29–45.

Berggren, W.A., Kent, D.V., Swisher, C.C., III, and Aubry, M.-P., 1995. A revised Cenozoic geochronology and chronostratigraphy. *In* Berggren, W.A., Kent, D.V., Aubry, M.-P., and Hardenbol, J. (Eds.), *Geochronology, Time Scales and Global Stratigraphic Correlation.* Spec. Publ.—SEPM, 54:129–212.

Bohaty, S.M., Scherer, R.P., and Harwood, D.M., 1998. Quaternary diatom biostratigraphy and palaeoenvironments of the CRP-1 drillcore, Ross Sea, Antarctica. *Terra Antart.,* 5:431–453.

Bohaty, S.M., Wise, S.W., Jr., Duncan, R.A., Moore, C.L., and Wallace, P.J., in press. Neogene diatom biostratigraphy, tephra stratigraphy, and chronology of ODP Hole 1138A, Kerguelen Plateau. *Proc. ODP, Sci. Results,* 183: College Station, TX (Ocean Drilling Program).

Censarek, B., and Gersonde, R., 2002. Miocene diatom biostratigraphy at ODP Sites 689, 690, 1088, 1092 (Atlantic sector of the Southern Ocean). *Mar. Micropaleontol.,* 45:309–356.

Ciesielski, P.F., 1983. The Neogene and Quaternary diatom biostratigraphy of subantarctic sediments, Deep Sea Drilling Project Leg 71. *In* Ludwig, W.J., Krasheninnikov, V.A., et al., *Init. Repts. DSDP,* 71 (Pt. 2): Washington (U.S. Govt. Printing Office), 635–666.

Domack, E., Jull, A.J.T., and Donahue, D.J., 1991. Holocene chronology for the unconsolidated sediments at Hole 740A: Prydz Bay, East Antarctica. *In* Barron, J., Larsen, B., et al., *Proc. ODP, Sci. Results,* 119: College Station, TX (Ocean Drilling Program), 747–750.

Domack, E., O'Brien, P.E., Harris, P.T., Taylor, F., Quilty, P.G., DeSantis, L., and Raker, B., 1998. Late Quaternary sedimentary facies in Prydz Bay, East Antarctica and their relationship to glacial advance onto the continental shelf. *Antarct. Sci.,*10:227–235.

Dumont, M.P., Baldauf, J.G., and Barron, J.A., 1986. *Thalassiosira praeoestrupii*—a new diatom species for recognizing the Miocene/Pliocene Epoch boundary in coastal California. *Micropaleontology,* 32:372–377.

Fenner, J., 1978. Cenozoic diatom biostratigraphy of the equatorial and southern Atlantic Ocean. *In* Perch-Nielsen, K., Supko, P.R., et al., *Init. Repts. DSDP,* 39 (Suppl., Pt. 2): Washington (U.S. Govt. Printing Office), 491–624.

Fenner, J., Schrader, H.-J., and Wienigk, H., 1976. Diatom phytoplankton studies in the southern Pacific Ocean: composition and correlation to the Antarctic Convergence and its paleoecological significance. *In* Hollister, C.D., Craddock, C., et al., *Init. Repts. DSDP,* 35: Washington (U.S. Govt. Printing Office), 757–813.

Florindo, F., Bohaty, S.M., Erwin, P.S., Richter, C., Roberts, A.P., Whalen, P., and Whitehead, J.M., in press. Magnetobiostratigraphic chronology of Cenozoic

sequences from ODP Sites 1165 and 1166, Prydz Bay, Antarctica. *Palaeogeogr., Palaeoclimat., Palaeoecol.*

Fryxell, G.A., and Hasle, G.R., 1972. *Thalassiosira eccentrica* (Ehrenberg) Cleve, *T. symmetrica* sp. nov., and some related Centric diatoms. *J. Phycol.,* 8:297–317.

Gersonde, R., 1991. Taxonomy and morphostructure of late Neogene diatoms from Maud Rise (Antarctic Ocean). *Polarforschung,* 59:141–171.

Gersonde, R., and Bárcena, M.A., 1998. Revision of the late Pliocene–Pleistocene diatom biostratigraphy for the northern belt of the Southern Ocean. *Micropaleontology,* 44:84–98.

Gersonde, R., and Burckle, L.H., 1990. Neogene diatom biostratigraphy of ODP Leg 113, Weddell Sea (Antarctic Ocean). *In* Barker, P.F., Kennett, J.P., et al., *Proc. ODP, Sci. Results,* 113: College Station, TX (Ocean Drilling Program), 761–789.

Gombos, A.M., 1976. Paleogene and Neogene diatoms from the Falkland Plateau and Malvinas Outer Basin: Leg 36, Deep Sea Drilling Project. *In* Barker, P., Dalziel, I.W.D., et al., *Init. Repts. DSDP,* 36: Washington (U.S. Govt. Printing Office), 575–687.

Hambrey, M.J., Ehrmann, W.U., and Larsen, B., 1991. Cenozoic glacial record of the Prydz Bay continental shelf, East Antarctica. *In* Barron, J., Larsen, B., et al., *Proc. ODP, Sci. Results,* 119: College Station, TX (Ocean Drilling Program), 77–132.

Harwood, D.M., 1989. Siliceous microfossils. *In* Barrett, P.J. (Ed.), *Antarctic Cenozoic History from the CIROS-1 Drillhole, McMurdo Sound.* DSIR Bull. N.Z., 245:67–97.

Harwood, D.M., and Bohaty, S.M., 2001. Early Oligocene siliceous microfossil biostratigraphy of Cape Roberts project Core CRP-3, Victoria Land Basin, Antarctica. *Terra Antart.,* 8:315–338.

Harwood, D.M., and Maruyama, T., 1992. Middle Eocene to Pleistocene diatom biostratigraphy of Southern Ocean sediments from the Kerguelen Plateau, Leg 120. *In* Wise, S.W., Jr., Schlich, R., et al., *Proc. ODP, Sci. Results,* 120: College Station, TX (Ocean Drilling Program), 683–733.

Harwood, D.M., McMinn, A., and Quilty, P.G., 2000. Diatom biostratigraphy and age of the Pliocene Sørsdal Formation, Vestfold Hills, East Antarctica. *Antarct. Sci.,* 12:443–462.

Johansen, J.R., and Fryxell, G.A., 1985. The genus *Thalassiosira* (Bacillariophyceae): studies on species occurring south of the Antarctic Convergence Zone. *Phycologia,* 24:155–179.

Koizumi, I., 1973. The late Cenozoic diatoms of Sites 183–193, Leg 19 Deep Sea Drilling Project. *In* Creager, J.S., Scholl, D.W., et al., *Init. Repts. DSDP,* 19: Washington (U.S. Govt. Printing Office), 805–855.

Mahood, A.D., and Barron, J.A., 1995. *Thalassiosira tetraoestrupii* var. *reimeri* var. nov., a distinctive diatom from the late Pliocene of the Southern Ocean. *In* Kociolek, J.P., and Sullivan, M.J. (Eds.), A *Century of Diatom Research in North America: A Tribute to the Distinguished Careers of Charles Reimer and Ruth Patrick:* Champaign, IL (Koeltz Sci. Books USA), 1–8.

————, 1996. Late Pliocene diatoms in a diatomite from Prydz Bay, East Antarctica. *Micropaleontology,* 42:285–302.

McCollum, D.W., 1975. Diatom stratigraphy of the southern Ocean. *In* Hayes, D.E., Frakes, L.A., et al., *Init. Repts. DSDP,* 28: Washington (U.S. Govt. Printing Office), 515–571.

McKelvey, B., Hambrey, M., Harwood, D., Mabin, M., Webb, P., Whitehead, J., 2001. The Pagodroma Group: the Neogene record in the northern Prince Charles Mountains of a dynamic Lambert Glacier and East Antarctic Ice Sheet. *Antarct. Sci.,* 13:455–468.

McMinn, A., and Harwood, D.M., 1995. Biostratigraphy and paleoecology of early Pliocene diatom assemblages from the Larsemann Hills, eastern Antarctica. *Antarct. Sci.,* 7:115–116.

Medlin, L.K., and Priddle, J. (Eds.), 1990. *Polar Marine Diatoms:* Cambridge (British Antarct. Surv.).

O'Brien, P.E., Cooper, A.K., Richter, C., et al., 2001. *Proc. ODP, Init. Repts.,* 188 [Online]. Available from World Wide Web: <http://www-odp.tamu.edu/publications/188_IR/188ir.htm>. [Cited 2002-07-01].

Priddle, J., and Fryxell, G.A., 1985. *Handbook of the Common Plankton Diatoms of the Southern Ocean: Centrales Except the Genus* Thalassiosira: Cambridge (Cambridge Univ. Press).

Quilty, P.G., Truswell, E.M., O'Brien, P.E., and Taylor, F., 1999. Paleocene–Eocene biostratigraphy and palaeoenvironment of East Antarctica: new data from Mac. Robertson Shelf and western Prydz Bay. *AGSO J. Aust. Geol Geophys.,* 17:133–143.

Roberts, D., and McMinn, A., 1999. Diatoms of the saline lakes of the Vestfold Hills, Antarctica. *Bib. Diatomol.,* 44:83.

Scherer, R.P., Bohaty, S.M., and Harwood, D.M., 2000. Oligocene and lower Miocene siliceous microfossil biostratigraphy of Cape Roberts Project core CRP-2/2A, Victoria Land Basin, Antarctica. *Terra Antart.,* 7:417–442.

Scherer, R.P., and Koç, N., 1996. Late Paleogene diatom biostratigraphy and paleoenvironments of the northern Norwegian-Greenland Sea. *In* Thiede, J., Myhre, A.M., Firth, J.V., Johnson, G.L., and Ruddiman, W.F. (Eds.), *Proc. ODP, Sci. Results,* 151: College Station, TX (Ocean Drilling Program), 75–99.

Schrader, H.-J., 1973. Cenozoic diatoms from the Northeast Pacific, Leg 18. *In* Kulm, L.D., von Huene, R., et al., *Init. Repts. DSDP,* 18: Washington (U.S. Govt. Printing Office), 673–797.

————, 1976. Cenozoic planktonic diatom biostratigraphy of the Southern Pacific Ocean. *In* Hollister, C.D., Craddock, C., et al., *Init. Repts. DSDP,* 35: Washington (U.S. Govt. Printing Office), 605–671.

Shipboard Scientific Party, 2001. Leg 188 summary: Prydz Bay-Cooperation Sea, Antarctica. *In* O'Brien, P.E., Cooper, A.K., Richter, C., et al., *Proc. ODP, Init. Repts.,* 188, 1–65 [CD-ROM]. Available from: Ocean Drilling Program, Texas A&M University, College Station TX 77845-9547, USA.

Stagg, H.M.J., 1985. The structure and origin of Prydz Bay and MacRobertson Shelf, East Antarctica. *Tectonophysics,* 114:315–340.

Taylor, F., and McMinn, A., 2002. Late Quaterrnary diatom assemblages from Prydz Bay, eastern Antarctica. *Quat. Res.,* 57:151–161.

Taylor, F., McMinn, A., and Franklin, D., 1997. Distribution of diatoms in surface sediments of Prydz Bay, Antarctica. *Mar. Micropaleontol.,* 32:209–229.

Whitehead, J.M., 2000. Cenozoic palaeoenvironment of the Southern Ocean and East Antarctica: geological and palaeontological evidence from the Kerguelen Plateau, Vestfold Hills and Prince Charles Mountains [Ph.D. dissert.]. Univ. Tasmania, 258.

Whitehead, J.M., and McKelvey, B.C., 2001. The stratigraphy of the Pliocene–lower Pleistocene Bardin Bluffs Formation, Amery Oasis, northern Prince Charles Mountains, Antarctica. *Antarct. Sci.,* 13: 79–86.

Whitehead, J.M., and McMinn, A., 1997. Paleodepth determination from Antarctic benthic diatom assemblages. *Mar. Micropaleontol.,* 29:301–318.

Winter, D., and Iwai, M., 2002. Data report: Neogene diatom biostratigraphy, Antarctic Peninsula Pacific margin, ODP Leg 178 rise sites. *In* Barker, P.F., Camerlenghi, A., Acton, G.D., and Ramsay, A.T.S. (Eds.), *Proc. ODP, Sci. Results,* 178 [Online]. Available from World Wide Web: <http://www-odp.tamu.edu/publications/178_SR/chap_29/chap_29.htm> [Cited 2002-11-20].

Winter, D.M., and Harwood, D.M., 1997. Integrated diatom biostratigraphy of late Neogene drillholes in Southern Victoria Land and correlation to Southern Ocean records. *In* Ricci, C.A. (Ed.), *The Antarctic Region: Geological Evolution and Processes.* Terra Antart. Publ., 985–992.

Yanagisawa, Y., and Akiba, F., 1990. Taxonomy and phylogeny of the three marine diatom genera, *Crucidenticula, Denticulopsis* and *Neodenticula. Bull. Geol. Surv. Jpn.,* 41:197–301.

Zielinski, U., and Gersonde, R., 2002. Plio-Pleistocene diatom biostratigraphy from ODP Leg 177, Atlantic sector of the Southern Ocean. *Mar. Micropaleontol.,* 45:225–268.

APPENDIX

Taxonomic List

Actinocyclus actinochilus (Ehrenberg) Simonsen, 1982; Fenner et. al., 1974, p. 771 (as *Charcotia actinochilus* [Ehrenberg] Hustedt), pl. 5, fig. 5.

Actinocyclus fasciculatus Harwood and Maruyama, 1992, p. 727, pl. 13, figs. 14, 15.

Actinocyclus ingens Rattray 1890; Harwood and Maruyama, 1992, p. 700, pl. 8, fig. 10; pl. 11, figs. 4, 6; pl. 12, fig. 8.

Actinocyclus aff. *ingens* Rattray, 1891; Schrader, 1973, p. 663, pl. 11, figs. 6, 7.

Actinocyclus karstenii Van Heurck, 1909; Harwood and Maruyama, 1992, p. 700, pl. 13, figs. 1, 2, 6–8, 11, 13.

Actinocyclus maccollumii Harwood and Maruyama, 1992, p. 700, pl. 17, fig. 29.

Actinocyclus fryxellae Barron, in Baldauf and Barron, 1991, p. 585, pl. 1, figs. 1, 2, 4.

Actinoptychus senarius Ehrenberg, 1838; Gombos, 1976, p. 655, pl. 26, figs. 1–3 (as *Actinoptychus undulatus* [Bailey] Ralfs).

Asteromphalus parvulus Karsten, 1905.

Azpeitia tabularis (Grunow) Fryxell and Sims, 1986; Akiba, 1982, p. 42, pl. 2, figs. 6–10.

Chaetoceros bulbosum (Ehrenberg) Heiden, 1928; Priddle and Fryxell, 1985, p. 25, fig. C.

Chaetoceros spp. Ehrenberg, 1844.
Remarks: This group includes cysts, setae, and rare vegetative forms.

Cocconeis spp. Ehrenberg, 1838.

Corethron criophilum Castracane, 1886; Harwood and Maruyama, 1992, p. 701, pl. 5, fig. 15; pl. 19, figs. 12–15.

Coscinodiscus marginatus Ehrenberg, Hustedt, 1930; Barron, 1981, p. 118, pl. 1, fig. 2.

Coscinodiscus spp. Ehrenberg, 1838.

Dactyliosolen antarcticus Castracane, 1886; Harwood and Maruyama, 1992, p. 702, pl. 18, fig. 12.

Denticulopsis delicata Yanagisawa and Akiba, 1990, p. 246, pl. 7, figs. 1–4.

Denticulopsis dimorpha (Schrader) Simonsen, 1979; Yanagisawa and Akiba, 1990, pp. 254–255, pl. 4, figs. 42–49; pl. 7, figs. 14–16.

Denticulopsis hustedtii (Simonsen and Kanaya) Simonsen, 1979; Yanagisawa and Akiba, 1990, pp. 246–248, pl. 3, figs. 15–16; pl. 11, figs. 11–13.

Denticulopsis lauta Simonsen, 1979; Yanagisawa and Akiba, 1990, pp. 235–236, pl. 2, figs. 6–8, 15; pl. 5, figs. 1–3; pl. 9, fig. 1.

Denticulopsis maccollumii Simonsen, 1979; Yanagisawa and Akiba, 1990, pp. 246–248, pl. 2, figs. 39–41.

Denticulopsis ovata (Schrader) Yanagisawa and Akiba, 1990, pp. 257–258, pl. 6, figs. 6–14, 24–32; Harwood and Maruyama, 1992, pp. 702–703, pl. 6, figs. 1–4; pl. 7, figs. 1–4, 6–9, 11–13; pl. 9, figs. 1–4, 10–14; pl. 10, fig. 7 (as *Denticulopsis meridonalis*).

Denticulopsis simonsenii Yanagisawa and Akiba, 1990, pp. 242–243, pl. 3, figs. 1–3; pl. 11, figs. 1–5.

Remarks: *Denticulopsis simonsenii* was separated from *Denticulopsis vulgaris* using the species concepts illustrated and described by Yanagisawa and Akiba (1990). *Denticulopsis simonsenii* is characterized by two full rows of aerolae between the psuedosepta, in contrast to *D. vulgaris,* which has rows of areolation on either side (and near) each psuedosepta.

Denticulopsis vulgaris (Okuno) Yanagisawa and Akiba, 1990, pp. 243, 244, pl. 3, figs. 4–8; pl. 11, figs. 6–10.
Remarks: See notes under *Denticulopsis simonsenii.*

Denticulopsis sp. 3.
Remarks: *Denticulopsis* sp. 3 has larger and fewer areolae than *D. simonsenii,* with an outer valve view similar to that of *Denticulopsis dimorpha* var. *areolata* Yanagisawa and Akiba (1990) under light microscope (e.g., Yanagisawa and Akiba 1990, p. 287, pl. 5, figs. 13, 14).

Diploneis bomboides (Schmidt) Cleve, 1894–1895; Roberts and McMinn, 1999, p. 21, pl. 3, fig. 1 (as *Diploneis splendidus* [Gregory] Cleve, 1894–1895).

Diploneis subovalis Cleve, 1894; Harwood et al., 2000, p. 459, pl. 9, fig. 1.

Diploneis spp. Ehrenberg, 1844.

Drepanotheca sp. Schrader, 1969.

Eucampia antarctica (Castracane) Mangin, 1914; Mahood and Barron, 1996, p. 290, pl. 2, figs. 1–3; pl. 7, figs. 1, 2.

Fragilariopsis arcula (Gersonde) Gersonde and Bárcena, 1998; Gersonde, 1991, pp. 142–144 (as *Nitzschia arcula* Gersonde 1991), pl. 2, fig. 4; pl. 4, fig. 4; pl. 5, figs. 1–6.

Fragilariopsis aurica (Gersonde) Gersonde and Bárcena, 1998; Harwood and Maruyama, 1992, pp. 144–146 (as *Nitzschia aurica* Gersonde 1991), pl. 1, figs. 18–25; pl. 3, fig. 5; pl. 4, figs. 5, 6; pl. 7, fig. 6.

Fragilariopsis barronii (Gersonde) Gersonde and Bárcena, 1998; Gersonde, 1991, pp. 146–147 (as *Nitzschia barronii* Gersonde 1991), pl. 3, fig. 6; pl. 4, figs. 1–3; pl. 5, figs. 7–17; Harwood and Maruyama, 1992, p. 704 (as *Nitzschia barronii*), pl. 17, figs. 27, 28.

Fragilariopsis barronii var. A and B of Whitehead, 2000 (as *Fragilariopsis barronii* var. A and B), pl. 5, figs 6–9.

Fragilariopsis curta (Van Heurck) Hasle, 1958; Harwood and Maruyama, 1992, p. 704, pl. 17, figs. 1–4 (as *Nitzschia curta* [Van Heurck] Hasle, 1972).

Fragilariopsis cylindrus (Grunow) Krieger, 1954; Medlin and Priddle, 1990, p. 181 (as *Nitzschia cylindrus* [Grunow] Hasle, 1972), pl. 24.6, figs. 6–11.

Fragilariopsis efferans (Schrader) Censarek and Gersonde; Schrader, 1976, p. 633 (as *Nitzschia efferans* Schrader 1976), pl. 2, figs. 1, 3, 5–7.

Fragilariopsis interfrigidaria (McCollum) Gersonde and Bárcena, 1998; Baldauf and Barron, 1991, p. 589 (as *Nitzschia interfrigidaria* McCollum, 1975), pl. 7, fig. 12.

Fragilariopsis kerguelensis (O'Meara) Hasle, 1952; Medlin and Priddle, 1990, p. 181 (as *Nitzschia kerguelensis* [O'Meara] Hasle, 1972), pl. 24.2, figs. 11–18; p. 187, pl. 24.3, fig. 9.
Remarks: Early forms of *F. kerguelensis* possess smaller areolae than typical modern forms and have been recorded as "early" within the range data.

Fragilariopsis lacrima (Gersonde) Gersonde and Bárcena, 1998; Gersonde, 1991, p. 148 (as *Nitzschia lacrima* Gersonde, 1991), pl. 1, figs. 1–6, 26; pl. 2, figs. 1–3.

Fragilariopsis matuyamae Gersonde and Bárcena, 1998, p. 93, pl. 1, figs. 1–9, 13–16; pl. 2, figs. 1, 4, 5, 7–9.

Fragilariopsis cf. *lineata* (Castracane) Hasle.
Remarks: This form resembles extant *Fragilariopsis lineata* under the light microscope.

Fragilariopsis obliquecostata (Van Heurck) Heiden in Heiden and Kolbe, 1928; Akiba 1982, p. 69, pl. 9, fig. 11.

Fragilariopsis cf. *obliquecostata* (Van Heurck) Heiden in Heiden and Kolbe, 1928.
Remarks: A heavily silicified form of *F. obliquecostata* was recorded as *F.* cf. *obliquecostata*.

Fragilariopsis praecurta (Gersonde) Gersonde and Bárcena, 1998; Harwood and Maruyama, 1992, p. 704 (as *Nitzschia praecurta* Gersonde, 1991), pl. 17, figs. 25, 26.

Fragilariopsis praeinterfrigidaria (McCollum) Gersonde and Bárcena, 1998; Barron, 1985, p. 805 (as *Nitzschia praeinterfrigidaria* McCollum, 1975), fig. 14, figs. 5, 6.

Fragilariopsis ritscheri Hustedt, 1958; Bohaty et al., 1998, pl. 1, fig. 8.

Fragilariopsis rhombica (O'Meara) Hustedt, 1952; Abbott 1974, p. 339, pl. 7, figs. D, E.

Fragilariopsis separanda var. A of Whitehead, 2000, pl. 5, figs. 14, 15.

Fragilariopsis sublinearis (Van Heurck) Heiden, 1928; Medlin and Priddle, 1990, pp. 181–182 (as *Nitzschia sublinearis* Hasle, 1972), pl. 14.5, figs. 1–10.

Fragilariopsis weaveri (Ciesielski) Gersonde and Bárcena, 1998; Ciesielski, 1983, p. 655 (as *Nitzschia weaveri* Ciesielski, 1983), pl. 1, figs. 1–10.

Fragilariopsis spp. Hustedt, 1913.

Hemiaulus polymorphus Grunow, 1884; Fenner, 1978, p. 522, pl. 21, fig. 11; pl. 22, figs., 4, 5, 7–10; pl. 23, figs. 1–4.

Hemiaulus spp. Ehrenberg, 1844.

Hemidiscus karstenii Jousé, 1962; Barron, 1985, p. 786, figs. 14, 20.

Isthmia spp. Agardh, 1832.

Liradiscus spp. Greville, 1865.

Navicula directa (Smith) Ralfs in Pritchard, 1861; Roberts and McMinn, 1999, p. 31, pl. 4, fig. 13.

Navicula spp. Bory, 1822.

Nitzschia grossepunctata Schrader, 1976; Gersonde and Burckle, 1990, p. 780, pl. 2, figs. 3–6.

Nitzschia reinholdii Kanaya in Barron and Baldauf, 1986; Gersonde and Burckle, 1990, p. 782, pl. 2, fig. 1.

Nitzschia spp. Hassall 1845.

Odontella weissflogii (Janisch) Grunow.

Paralia spp. Heiberg, 1863.

Pinnularia spp. Ehrenberg, 1841.

Porosira psuedodenticulata (Hustedt) Jousé, 1962.

Proboscia barboi (Brün) Jordan and Priddle, 1991; Harwood and Maruyama, 1992, p. 706 (as *Simonseniella barboi* [Brün] Fenner), pl. 11, fig. 13.

Proboscia sp. A.
Remarks: This form possesses long apices that are broadly rounded.

Pyxilla reticulata Grove and Sturt, 1887; Harwood and Bohaty, 2001, p. 329, pl. 4, figs. 1, 3, 4, 9.

Pyxilla spp. Greville, 1865.

Rhizosolenia costata Gersonde, 1991, p. 149–150, pl. 9, figs. 1–6.

Rhizosolenia hebetata group Bailey, 1856; Koizumi, 1973, p. 833, pl. 5, fig. 35.
Remarks: This group consists of *Rhizosolenia* spp. lacking otaria.

Rhizosolenia hebetata f. *hiemalis-spinosa* Gran sensu Schrader, 1976, p. 635, pl. 9, fig 3.
Remarks: This form is finer in structure and less heavily silicified than *Rhizosolenia hebetata* f. *hiemalis*.

Rhizosolenia hebetata f. *hiemalis* Grun, 1904.
Remarks: This form appears more hyaline toward the apices and possesses reduced areolation compared to *R. hebetata* f. *hiemalis-spinosa* forms noted in the current study.

Rhizosolenia oligocaenica Schrader, 1976, p. 635, pl. 9, fig. 7.

Rhizosolenia styliformis group Brightwell, 1858; Harwood and Maruyama, 1992, p. 705, pl. 18, fig. 20.
Remarks: This group consists of *Rhizosolenia* spp. with otaria.

Rhizosolenia sp. A.
Remarks: This form is similar to *R. hebetata* but possesses curved apices.

Rhizosolenia sp. D of Harwood and Maruyama, 1992, p. 705, pl. 18, figs. 7, 8.

Rouxia antarctica (Heiden) Hanna, 1930; Bohaty et al., 1998, pl. 1, fig 7.

Rouxia diploneides Schrader, 1973; Harwood and Maruyama, 1992, p. 705, pl. 17, fig. 12.

Rouxia heteropolara Gombos, 1974; Gersonde and Burckle, 1990, p. 782, pl. 5, fig. 2.

Rouxia isopolica Schrader, 1976, pp. 635–636, pl. 5, figs. 9, 14, 15, 20.

Rouxia naviculoides Schrader, 1973, p. 710, pl. 3, figs. 27–32.

Rouxia spp. Brün and Heribaud, 1893.

Stephanopyxis turris (Greville and Arnott) Ralfs in Pritchard, 1861; Harwood, 1989, p. 81, pl. 2, figs. 21–23.

Stephanopyxis spp. Ehrenberg, 1845.

Stellarima microtrias (Ehrenberg) Hasle and Sims, 1986; Harwood, 1989, p. 80, pl. 1, fig. 4.

Stellarima stellaris (Roper) Hasle and Sims, 1986; Harwood, 1989, p. 80, pl. 1, fig. 3.

Synedra sp. A.
Remarks: Valve length = 30 µm, width = ~3–4 µm, and apices are broadly rostrate.

Synedropsis sp. A Scherer et al., 2000, p. 440, pl. 2, fig. 14 (as *"Tigeria"* sp. A).

Synedropsis sp. B Scherer et al., 2000, p. 440, pl. 2, figs. 15, 16 (as *"Tigeria"* sp. B and C).

Synedropsis sp. C Harwood and Maruyama, 1992, p. 706 (as *Synedra* sp. 1), pl. 17, figs. 6, 7.
Remarks: Valves are triundulate in outline.

Synedropsis spp. Hasle et al.

Thalassionema nitzschioides var. 1 of Bohaty et al., in press.

Remarks: This variety has one spatulate-shaped apice.

Thalassionema spp. Grunow in Van Heurck, 1881.

Thalassiosira antarctica Comber, 1896; Roberts and McMinn, 1999, p. 48, pl. 9, figs. 3, 4.

Thalassiosira complicata Gersonde, 1991; Harwood and Maruyama, 1992, p. 707, pl. 14, figs. 18–21.

Thalassiosira cf. *eccentrica* (Ehrenberg) Cleve; Fryxell and Hasle, 1972, p. 300, figs. 1–18.

Thalassiosira elliptipora (Donahue) Fenner in Mahood and Barron, 1996, pp. 292–294, pl. 4, fig. 3; pl. 5, figs. 4a–7c; pl. 8, fig. 8; Harwood and Maruyama, 1992, p. 707, pl. 16, fig. 12.

Thalassiosira fasciculata Harwood and Maruyama, 1992, p. 729, pl. 15, figs. 4–6.

Thalassiosira gracilis var. *gracilis* (Karsten) Hustedt, 1958; Johansen and Fryxell, 1985, pp. 168–170, figs. 58, 59.

Thalassiosira insigna (Jousé) Harwood and Maruyama, 1992, p. 707, pl. 14, figs. 3–5.

Thalassiosira inura/insigna "intermediate forms" Harwood and Maruyama, 1992, p. 707, pl. 14, figs. 7–10.

Thalassiosira inura Gersonde, 1991; Harwood and Maruyama, 1992, p. 707, pl. 5, fig. 14; p. 728, pl. 14, figs. 12–14, 16.
Remarks: In the present study, *T. inura* is limited to specimens with a central hyaline patch that spans at least one-fourth of the valve diameter.

Thalassiosira jacksonii Koizumi and Barron in Koizumi; Baldauf and Barron, 1991, p. 591, pl. 6, fig. 7.
Remarks: *Thalassiosira jacksonii* is present below the first occurrence of *T. inura,* and we differentiate *T. jacksonii* by its finer areolation and reduced central hyaline area compared to *T. inura*.

Thalassiosira kolbei (Jousé) Gersonde, 1990; McCollum, 1975, p. 527 (as *Coscinodiscus kolbei* Jousé, 1962), pl. 4, figs. 7–9.

Thalassiosira lentiginosa (Janisch) Fryxell, 1977; Johansen and Fryxell, 1985, p. 170, figs. 49, 50.

Thalassiosira maculata Johansen and Fryxell, 1985, p. 170, figs. 72–74.

Thalassiosira miocenica Schrader; Baldauf and Barron, 1991, p. 591, pl. 6, fig. 2.

Thalassiosira nansenii Scherer and Koç, 1996, p. 89, pl. 4, figs. 1–5.

Thalassiosira oliverana (O'Meara) Makarova and Nikolaev, 1983; Abbott, 1974, p. 319, pl. 2, figs. D–F.

Thalassiosira oliverana "coarse" (O'Meara) Makarova, sensu Harwood and Maruyama, 1992, p. 708, pl. 14, figs. 6, 11.

Thalassiosira oliverana var. *sparsa* Harwood and Maruyama, 1992, p. 708, pl. 16, fig. 13.

Thalassiosira praefraga Gladekov and Barron, 1995; Scherer et al., 2000, p. 440, pl. 2, figs. 3, 7.

Thalassiosira praeoestrupii Dumont et al., 1986, p. 373, pl. 1, figs. 1–12.

Thalassiosira ritscheri (Hustedt) Hasle, 1968; Johansen and Fryxell, 1985, p. 176, figs. 14, 56, 57.

Thalassiosira striata Harwood and Maruyama, 1992, p. 708, pl. 15, figs. 7–9.

Thalassiosira tetraoestrupii Bodén, 1993; Mahood and Barron, 1995, figs. 9–19, 25, 26, 28–46.

Thalassiosira tetraoestrupii var. *reimeri* Mahood and Barron, 1995, figs. 1–8.

Thalassiosira torokina Brady, 1971; Mahood and Barron, 1996, p. 296, pl. 6, figs. 1–3.

Thalassiosira tumida (Janisch) Hasle in Heimdal and Fryxell, 1971; Johansen and Fryxell, 1985, p. 176, figs. 28–32.

Thalassiosira vulnifica (Gombos) Fenner, 1991; Harwood and Maruyama, 1992, p. 708, pl. 15, fig 1.

Thalassiosira spp. Cleve, 1873.

Thalassiothrix spp. Cleve and Grunow, 1880.

Trachyneis aspera (Ehrenberg) Cleve, 1984; Roberts and McMinn, 1999, p. 44, pl. 7, fig. 9.

Trichotoxon spp. Reid and Round, 1987.

Triceratium spp. Ehrenberg et al., 1839.

Trinacria excavata Heiberg, 1863; Harwood, 1989, p. 82, pl. 3, fig. 1.

Figure F1. Prydz Bay, Wild Drift, and other locations referred to in this report.

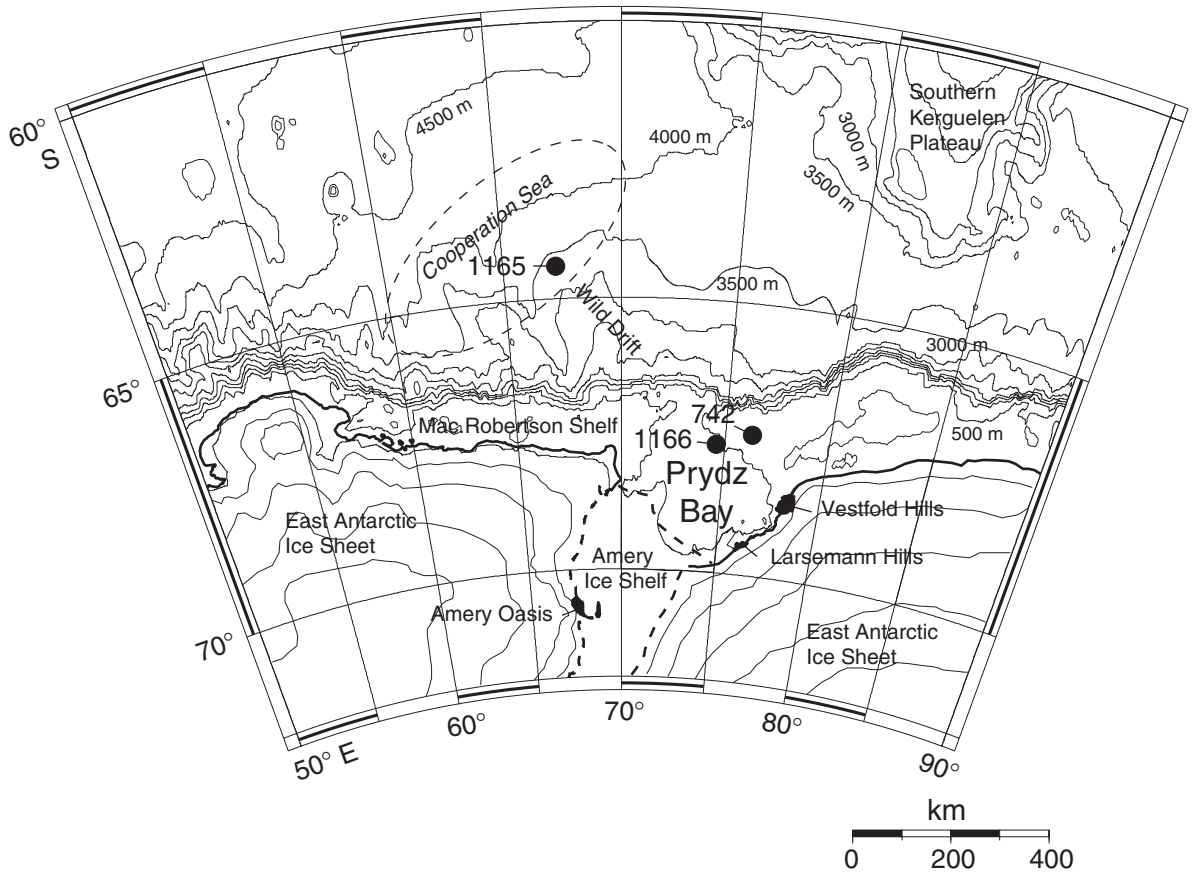

Table T1. Key diatom datums used for Pliocene–Pleistocene strata.

Datum	Present		Absent		Average depth (mbsf)	Depth error (±m)	Age (Ma)	Source(s)
	Core, section, interval (cm)	Depth (mbsf)	Core, section, interval (cm)	Depth (mbsf)				
	188-1165B-		188-1165B-					
LO *Actinocyclus ingens*	1H-4, 20–21	4.70	1H-2, 20–21	1.70	3.20	1.50	0.38	ZG
LO *Fragilariopsis barronii*	2H-2, 20–21	8.50	1H-CC, 15–20	6.81	7.66	0.85	1.2–1.5	BB, HM, GB, ZG
LO *Thalassiosira kolbei*	3H-1, 95–96	17.25	2H-2, 95–96	9.25	13.25	4.00	1.8–2.0	BB, HM, ZG
LO *Thalassiosira vulnifica*	3H-1, 95–96	17.25	3H-1, 77–80	17.07	17.16	0.09	2.1–2.5	ZG, WI
LO *Thalassiosira insigna*	3H-1, 117–120	17.47	3H-1, 95–96	17.25	17.36	0.11	2.5–2.7	WI
LO *Fragilariopsis weaveri*	3H-1, 95–96	17.25	3H-1, 77–80	17.07	17.16	0.09	2.5–2.7	ZG
FO *Thalassiosira vulnifica*	3H-CC	25.01	4H-1, 6–8.5	25.86	25.44	0.42	2.7–3.2	BB, HM, WI
FO *Fragilariopsis weaveri*	4H-1, 125–126	27.05	4H-2, 125–126	28.55	27.80	0.75	3.4–3.5	ZG
FO *Fragilariopsis interfrigidaria*	5H-2, 127–129.5	38.07	5H-3, 95–96	38.05	38.06	0.59	3.7–3.8	BB, HM, WI, ZG
FO *Fragilariopsis barronii*	5H-5, 47–50	41.77	5H-5, 60–61	41.90	41.84	0.06	4.2–4.3	BB, WI
FO *Thalassiosira inura*	6H-4, 95–96	50.25	6H-5, 59–60	51.39	50.82	0.57	4.8–5.0	BB, CG
	188-1166A-		188-1166A-					
LO *Actinocyclus ingens*	1R-CC	3.02	1R-2, 72–73	2.22	2.62	0.40	0.38	ZG
LO *Thalassiosira kolbei*	13R-1, 65–66	113.95	(Preservation)	—			>1.8–2.0	BB, HM, ZG
LO *Thalassiosira vulnifica*	13R-1, 123–124	114.53	13R-1, 80–83	114.10	114.32	0.22	2.1–2.5	ZG, WI
LO *Thalassiosira insigna*	13R-1, 124–126	114.54	13R-1, 80–83	114.10	114.32	0.22	2.5–2.7	WI
FO *Thalassiosira vulnifica*	13R-2, 65–67	115.45	(Preservation)	117.25	116.35	0.90	<2.7–3.2	BB, HM, WI
FO *Thalassiosira elliptipora*	13R-CC	117.25	(Preservation)	—			<~3.0	WH

Notes: LO = last occurrence, FO = first occurrence. BB = Baldauf and Barron (1991). HM = Harwood and Maruyama (1992). ZG = Zielinski and Gersonde (in press); datums south of Subantarctic Front. GB = Gersonde and Bárcena (1998). WI = Winter and Iwai (2002). CG = Censarek and Gersonde (in press). WH = Winter and Harwood (1997).

Table T2. Diatoms, Hole 1165B. (This table is available in an **oversized format.**)

Table T3. Diatoms, Hole 1166A. (Continued on next page.)

Zone	Core, section, interval (cm)	Depth (mbsf)	Overall preservation	Overall abundance	*Actinocyclus actinochilus*	*Actinocyclus fasciculatus*	*Actinocyclus ingens*	*Actinocyclus karstenii*	*Asteromphalus parvulus*	*Azpeitia tabularis*	*Chaetoceros* spp.	*Cocconeis* spp.	*Corethron criophilum*	*Coscinodiscus* spp.	*Dactyliosolen antarcticus*	*Diploneis* spp.	*Eucampia antarctica*	*Fragilariopsis barronii*	*Fragilariopsis curta*	*Fragilariopsis cylindrus*	*Fragilariopsis kerguelensis*	*Fragilariopsis obliquecostata*	*Fragilariopsis rhombica*	*Fragilariopsis ritscheri*	*Fragilariopsis separanda*	*Fragilariopsis sublinearis*	*Isthmia* spp.	*Odontella weisfloggii*	*Porosira pseudodenticulata*	*Rhizosolenia hebetata* "group"	*R. hebetata* f. *hiemalis-spinosa*	*Rhizosolenia styliformis* "group"	*Rhizosolenia* sp. D	*Rouxia antarctica*	*Rouxia diploneides*	*Rouxia isopolica*	*Rouxia* spp.	*Stellarima microtrias*	*Stellarima stellaris*	*Thalassionema* spp.	*Thalassiosira antarctica*	*Thalassiosira elliptipora*	*Thalassiosira fasciculata*	*Thalassiosira gracilis* var. *gracilis*
	188-1166A-																																									
T. lentiginosa	1R-2, 72–72.5	2.22	M–G	A	F						R				R		F		C	R	C	C	C		R	F			R									C			F
	1R-CC, 23–28	3.02	M	F	R				R	R	R			R	R	R	F				F	F		R	R			R									F			
Unzoned	2R-2, 24–25	10.64	P	Tr										R			R				R																				
Barren	3R-2, 27–29	21.57	—	—																																					
Barren	4R-1, 8–11	29.28	—	—																																					
Barren	5R-CC, 0–5	39.55	—	—																																					
Barren	6R-CC, 0–10	47.30	—	—																																					
Barren	7R-CC, 0–10	56.40	—	—																																					
Barren	8R-1, 77–82	66.17	—	—																																					
Barren	9R-CC, 8–18	76.10	—	—																																					
Barren	10R-CC, 15–20	85.13	—	—																																					
Barren	11R-CC, 26–31	95.70	—	—																																					
Barren	13R-1, 6–7	113.36	—	—																																					
Barren	13R-1, 29–31	113.59	—	—																																					
Barren	13R-1, 54–56	113.84	—	—																																					
	13R-1, 65–66	113.95	G	A		R		F			R	R	R				R							F		R				R			R	R		R	F		R			
T. kolbei	13R-1, 70–71	114.00	G	A		R		F			R	R			R		R		R					F		R				R		R				R	F				
	13R-1, 77–78	114.07	G	A		C		R			C						F		R			C								R		R	R	C			R		F	R	
	13R-1, 80–83	114.10	G	A		R							R		R														R			R	C	R			R		R		
Barren	13R-1, 91–93	114.21	—	—																																					
Barren	13R-1, 115–117	114.45	—	—																																					
	13R-1, 123–124	114.53	G	A		F		R					R		R		R	R				F		F		R	R			R			F	R			R		R		
Unzoned	13R-2, 8–10	114.88	G	A		F	C	R			R			R	R		F		R			C					R			R		R	C	R			R		F		
	13R-2, 65–67	115.45	G	A		R		F							R		R		R			F		F		R	R			R		R	C	R			R		R		
	13R-2, 74–76	115.54	P	Tr																																					
Unzoned	13R-2, 18–20	116.48	P	Tr																																					
	13R-2, 24–25	116.54	P	Tr																																					
Barren	13R-2, 34–35	116.64	—	—																																					

Notes: Preservation: G = good, M = moderate, P = poor. Abundance: A = abundant, C = common, F = few, R = rare, Tr = trace.

Table T3 (continued).

Zone	Core, section, interval (cm)	Depth (mbsf)	Overall preservation	Overall abundance	*Thalassiosira insigna*	*T. insigna/T. inura* "intermediate"	*Thalassiosira inura*	*Thalassiosira kolbei*	*Thalassiosira lentiginosa*	*Thalassiosira maculata*	*Thalassiosira oliverana* "coarse"	*Thalassiosira oliverana*	*Thalassiosira praeoestrupii*	*Thalassiosira tetraoestrupii*	*T. tetraoestrupii* var. *reimeri*	*Thalassiosira torokina*	*Thalassiosira tumida*	*Thalassiosira vulnifica*	*Trachyneis aspera*	*Trichotoxon* spp.
	188-1166A-																			
T. lentiginosa	1R-2, 72–72.5	2.22	M–G	A					F								F			
	1R-CC, 23–28	3.02	M	F					R			R				F				
Unzoned	2R-2, 24–25	10.64	P	Tr												R				
Barren	3R-2, 27–29	21.57	—	—																
Barren	4R-1, 8–11	29.28	—	—																
Barren	5R-CC, 0–5	39.55	—	—																
Barren	6R-CC, 0–10	47.30	—	—																
Barren	7R-CC, 0–10	56.40	—	—																
Barren	8R-1, 77–82	66.17	—	—																
Barren	9R-CC, 8–18	76.10	—	—																
Barren	10R-CC, 15–20	85.13	—	—																
Barren	11R-CC, 26–31	95.70	—	—																
Barren	13R-1, 6–7	113.36	—	—																
Barren	13R-1, 29–31	113.59	—	—																
Barren	13R-1, 54–56	113.84	—	—																
	13R-1, 65–66	113.95	G	A		R	R	R		R	R			R			R			R
T. kolbei	13R-1, 70–71	114.00	G	A		R		R	R		R			F		F			R	R
	13R-1, 77–78	114.07	G	A		F		F	F		F		F	R		F	F			R
	13R-1, 80–83	114.10	G	A		R			R	R	F			R		F				
Barren	13R-1, 91–93	114.21	—	—																
Barren	13R-1, 115–117	114.45	—	—																
	13R-1, 123–124	114.53	G	A		R				R	F		?	R		C	R	R		
Unzoned	13R-2, 8–10	114.88	G	A	R	R	R	F	F		F		R	R		C		F		
	13R-2, 65–67	115.45	G	A						R	F			R		F		R		
	13R-2, 74–76	115.54	P	Tr																
Unzoned	13R-2, 18–20	116.48	P	Tr																
	13R-2, 24–25	116.54	P	Tr																
Barren	13R-2, 34–35	116.64	—	—																

Table T4. Reworked diatoms and sponge spicules, Hole 1165B. (See table notes. Continued on next page.)

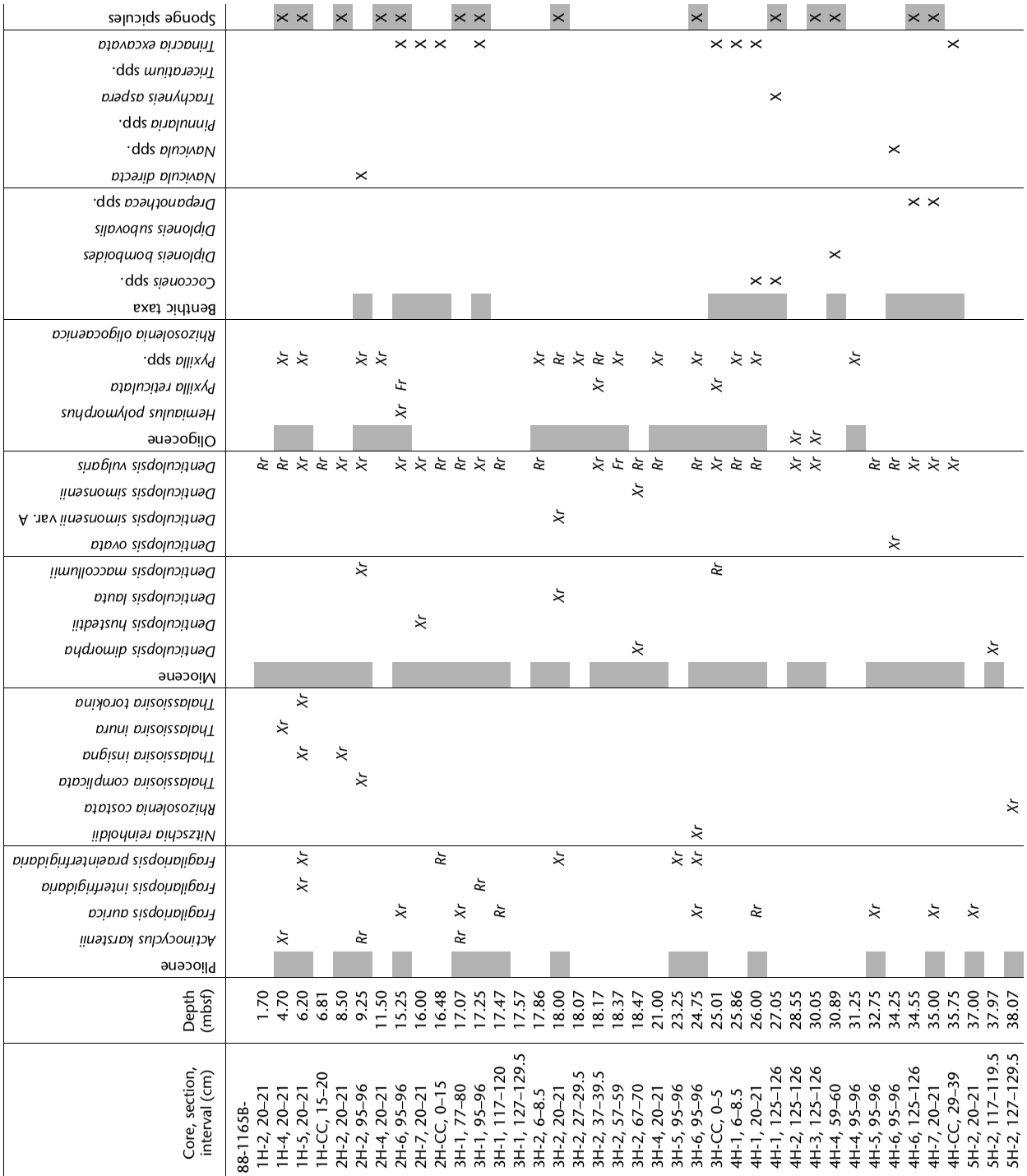

See table notes. Continued on next page.

Table T4 (continued).

Zone	Core, section, interval (cm)	Depth (mbsf)	Pliocene	*Actinocyclus karstenii*	*Fragilariopsis aurica*	*Fragilariopsis interfrigidaria*	*Fragilariopsis praeinterfrigidaria*	*Nitzschia reinholdii*	*Rhizosolenia costata*	*Thalassiosira complicata*	*Thalassiosira insigna*	*Thalassiosira inura*	*Thalassiosira torokina*	Miocene	*Denticulopsis dimorpha*	*Denticulopsis hustedtii*	*Denticulopsis lauta*	*Denticulopsis maccollumii*	*Denticulopsis ovata*	*Denticulopsis simonsenii* var. A	*Denticulopsis simonsenii*	*Denticulopsis vulgaris*	Oligocene	*Hemiaulus polymorphus*	*Pyxilla reticulata*	*Pyxilla* spp.	*Rhizosolenia oligocaenica*	Benthic taxa	*Cocconeis* spp.	*Diploneis bomboides*	*Diploneis subovalis*	*Drepanotheca* spp.	*Navicula directa*	*Navicula* spp.	*Pinnularia* spp.	*Trachyneis aspera*	*Triceratium* spp.	*Trinacria excavata*	Sponge spicules
	5H-3, 95–96	39.25			*Rr*																																	
	5H-4, 60–61	40.40							*Xr*													*Xr*																
F. barronii	5H-4, 95–96	40.75			*Xr*				*Xr*									*Xr*				*Xr*																
	5H-4, 107–109.5	40.87							*Rr*																													
	5H-5, 47–50	41.77																		X		*Xr*					*Xr*			X								
	5H-5, 60–61	41.90													*Xr*							*Rr*																
	5H-6, 20–21	43.00																				*Rr*								X								
	5H-6, 60–61	43.40													*Xr*					X		*Xr*																R
	5H-6, 95–96	43.75																												X								
	5H-CC, 21–31	44.08																				*Rr*																
	6H-1, 5–6	44.85																																				
T. inura	6H-1, 95–96	45.75																				*Xr*																
	6H-2, 95–96	47.25																																			X	X
	6H-4, 27–30	49.57																				*Rr*																
	6H-4, 37–40	49.67																		X																		
	6H-4, 59–60	49.89																				*Rr*															R	X
	6H-4, 95–96	50.25																													X			X				
	6H-5, 59–60	51.39																																				
	6H-5, 70–75	51.50																				*Xr*			*Xr*													
T. oestrupii	6H-6, 20–21	52.50																				*Rr*				*Xr*											X	X
	6H-7, 20–21	54.00																								*Xr*											R	X
	6H-CC, 16–26	54.39																				*Rr*					*Xr*											

Notes: Abundance: F = few, R = rare, X = present. Those abundance datums accompanied by an "r" are out of their known biostratigraphic ranges and are interpreted as reworked.

Table T5. Diatom datums, Hole 1165B.

Datum	Present		Absent		Average depth (mbsf)	Possible depth error (±m)	Age (Ma)		
	Core, section, interval (cm)	Depth (mbsf)	Core, section, interval (cm)	Depth (mbsf)			Upper	Lower	Average
	188-1165B-		188-1165B-						
FO *Thalassiosira vulnifica*	3H-CC	25.01	4H-1, 6.0–8.5	25.86	25.44	0.42	3.20	3.22	3.21
FO *Thalassiosira insigna*	3H-CC	25.01	4H-1, 6.0–8.5	25.86	25.44	0.42	3.20	3.22	3.21
FO *Fragilariopsis weaveri*	4H-1, 125–126	26.00	4H-2, 125–126	27.05	26.53	0.53	3.24	3.28	3.26
FO *Fragilariopsis interfrigidaria*	5H-2, 127–129.5	38.07	5H-3, 95–96	38.05	38.06	0.59	3.75	3.88	3.81
FO *Fragilariopsis barronii*	5H-5, 47–50	41.77	5H-5, 60–61	41.90	41.84	0.06	4.15	4.16	4.15
FO *Thalassiosira inura*	6H-4, 95–96	50.25	6H-5, 59–60	51.39	50.82	0.57	5.03	5.09	5.06

Note: FO = first occurrence.